CSIRO PUBLISHING
Soil Research, 2017, **55**, 809–818
http://dx.doi.org/10.1071/SR16182

Carbon and nitrogen molecular composition of soil organic matter fractions resistant to oxidation

Katherine Heckman[A,C], *Dorisel Torres*[B], *Christopher Swanston*[A], *and Johannes Lehmann*[B]

[A]USDA Forest Service, Northern Research Station, 410 MacInnes Drive, Houghton, MI 49931, USA.
[B]Soil and Crop Sciences, Cornell University, Ithaca, NY 14853, USA.
[C]Corresponding author. Email: kaheckman@fs.fed.us

Abstract. The methods used to isolate and characterise pyrogenic organic carbon (PyC) from soils vary widely, and there is little agreement in the literature as to which method truly isolates the most chemically recalcitrant (inferred from oxidative resistance) and persistent (inferred from radiocarbon abundance) fraction of soil organic matter. In addition, the roles of fire, fuel type and soil morphology in the preservation of PyC are not yet defined. In an attempt to elucidate the importance of oxidative recalcitrance, fuel type and soil morphology to the persistence of soil organic matter, we examined two strongly contrasting soils using a variety of PyC isolation techniques coupled with quantifications of the molecular structure and mean residence time of the isolated organic materials. Surface and subsurface soil samples were examined from a Red Chromosol soil and a Black Vertosol soil. The $\delta^{13}C$ values suggest that PyC in the Red Chromosol was sourced from eucalyptus, whereas PyC in the Black Vertosol was formed from grass. Soils were sieved at 53 μm, treated with hydrofluoric acid to remove organics associated with mineral surfaces, then subjected to three common 'PyC isolation' treatments: chromic acid, photo-oxidation and chromic acid followed by photo-oxidation. Molecular structure of the organic residues remaining after each treatment was quantified by solid-state ^{13}C cross polarisation magic angle spinning nuclear magnetic resonance and near edge X-ray absorption fine structure spectroscopy, and the mean residence time of the organic residues was estimated based on radiocarbon abundance. In all cases, treatment with chromic acid followed by photo-oxidation isolated the smallest proportion of organic matter (5–10% of <53 μm C) which also had the longest mean residence time (estimated 600–3460 years). Additionally, molecular structure measurements indicated that this fraction was not composed solely of aromatic compounds, suggesting a non-homogenous source for the most oxidative-resistant fraction of soil organic matter.

Additional keywords: chromic acid, photo-oxidation, pyrogenic carbon, soil organic matter.

Received 12 July 2016, accepted 20 May 2017, published online 23 June 2017

Introduction

The char residues of fire are ubiquitous in terrestrial and marine ecosystems (Bird *et al.* 2015) and contain variable proportions of pyrogenic carbon (PyC) (Cohen-Ofri *et al.* 2006). Due to its fused aromatic nature, PyC persists in the environment for extended periods and is recognised as an integral part of the soil organic C pool (Schmidt and Noack 2000; Knicker 2011*a*). PyC found in environmental samples varies in molecular structure, elemental composition and surface chemistry depending on fuel type, combustion temperature and depositional environment, among other factors (González-Pérez *et al.* 2004; Czimczik and Masiello 2007). Pyrogenic nitrogen (PyN), or N contained in pyrogenic organic matter has received less examination than PyC, although it also has been shown to vary in form and abundance with the abovementioned factors (Knicker 2007).

Quantification of the size and mean residence time of the PyC pool in soils is crucial to terrestrial C cycle modelling efforts, and a variety of methods of isolation exist. Comparative studies and review articles have illustrated that PyC quantity and composition vary strongly among isolation techniques (Schmidt and Noack 2000; Schmidt *et al.* 2001; Song *et al.* 2002; Hammes *et al.* 2007).

Previous work by Krull *et al.* (2006) explored the chemical nature and radiocarbon signature (as a proxy of mean residence time) of fractions extracted through a variety of common procedures, all assumed to isolate PyC with a highly condensed polyaromatic structure. The techniques employed included chromic acid oxidation (CrA) (Masiello and Druffel 1998), high-energy ultraviolet photo-oxidation (PO) (Skjemstad *et al.* 1993; Skjernstad *et al.* 1999), and 6 M hydrochloric acid (HCl) hydrolysis (Martel and Paul 1974; Leavitt *et al.* 1996). These techniques work on the general assumption that the fraction of soil organic matter (SOM) most resistant to oxidation or hydrolysis will be both polyaromatic and representative of the 'inert' or 'passive' fraction of SOM. Krull *et al.* (2006) indicated that these assumptions are not well founded. Examination of the residues produced by the techniques above yielded three main insights: (i) standard oxidation techniques meant to isolate PyC in soils (CrA, PO and HCl) actually isolate a combination of polyaromatic compounds and lipids, which often results in isolation of solely

lipids if no PyC is present in the soil; (ii) each technique yielded a residue with a unique mean residence time, which is not always longer than that of the untreated material, suggesting that oxidation cannot reliably be used to isolate the passive fraction of SOM; and (iii) molecular recalcitrance, as asserted by resistance to experimental oxidation, preserves SOM from biodegradation for longer periods than sorption to mineral surfaces in the soils examined. Krull *et al.* (2006) additionally drew comparisons between oxidative residues from soils with high and low fire-frequency. The most aggressive oxidative treatment, CrA followed by PO, isolated mostly lipids in ecosystems unaffected by fires but isolated mostly polyaromatic compounds in ecosystems with high fire-frequency. The question of whether the polyaromatic compounds isolated from the soils of high fire-frequency ecosystems were derived mostly from recent fire events or were representative of the 'passive' fraction of SOC was confounded by the presence of 'bomb C' (i.e. elevated radiocarbon signatures associated with aboveground thermonuclear testing).

The current study follows from the work of Krull *et al.* (2006) outlined above, and further explores the relationships among oxidative resistance, molecular structure and mean residence time, as well as the influence of soil morphology and fuel type on oxidative resistance. In order to eliminate variance associated with fire frequency and the presence of 'bomb C', the current study utilises two soils sampled before aboveground nuclear testing (1951) from two sites that had decadal fire frequencies. Prior to isolation of the oxidative-resistant fraction (assumed to be PyC), soils were treated with hydrofluoric acid (HF) to remove as much mineral-associated C as possible, thereby allowing the examination of only the PyC fraction of SOM preserved primarily through chemical recalcitrance against oxidation, not association with minerals. Based on the previous work examining the specificity of PyC isolation techniques outlined above, three oxidation treatments were selected for the current study: CrA, PO and CrA+PO. After application of the oxidation treatments, the molecular structure of the isolated organic material was measured by two independent techniques: nuclear magnetic resonance (^{13}C NMR) spectroscopy and near edge X-ray absorption fine structure (NEXAFS) spectroscopy. Estimates of molecular structure were then combined with metrics of mean residence time (^{14}C abundance) and particle surface characteristics (scanning electron microscopy (SEM) imaging) in an effort to address the following hypotheses: (i) PyC derived from wood and preserved within an iron (Fe)-rich soil will persist for longer periods than PyC derived from grass and preserved within a soil rich in shrink/swell clays; (ii) increasing N concentration in pyrogenic organic matter will be associated with shorter periods of preservation in soil; and (iii) PyC most resistant to oxidation will be richest in condensed aromatic structures and will have the longest period of persistence in soils.

Methods

Soils examined

Two 'pre-bomb' archived soil profiles were examined in the current study, a Red Chromosol soil and a Black Vertosol soil. Soils were sampled in 1951 from sites located just outside Brisbane, Australia, by the CSIRO Division of Soils, and were described and classified according to the Australian soil classification system (Isbell 2002). Archived soils collected before 1955 (often referred to as the 'pre-bomb' period) were used to prevent the interference of elevated atmospheric radiocarbon concentrations resulting from aboveground thermonuclear arms testing in the 1950s and 1960s on the interpretation of oxidative residues' radiocarbon signature. One surface and one subsurface sample were examined from each soil profile. Only a limited number of archived horizons were available, so sample depths differed between the two soils. The Red Chromosol soil was classified as a Haplic Mesotrophic Red Chromosol, and the Black Vertosol soil as an Epicalcareous Epipedal Black Vertosol. General bulk soil characteristics are given in Table 1. Site descriptions from the year of sampling (1951) indicate the presence of C_4 grasses and eucalypts at both sites. However, tree and shrub abundance was higher at the Red Chromosol site than at the Black Vertosol site, whereas grass abundance was greater at the Black Vertosol than the Red Chromosol. Both sites experienced decadal burning and had well-developed soils with an abundance of secondary minerals at the time of sampling. The Red Chromosol soil was formed in a crest position from eroded lateritic material; the site consisted of low hills. The Black Vertosol developed from actively agrading floodplain alluvium sourced from the Lockyer River.

Soils were selected based on their similarity to soils used in the preceding study (Krull *et al.* 2006), and also based on differences in morphology and site characteristics. A woodland-dominated vs grassland-dominated site leads to differences in fire fuel characteristics, and therefore possible differences in the morphology and chemistry of charred materials introduced to the soils. Differences in soil mineralogy and morphology, for example an abundance of stable oxides in the Red Chromosol soil vs a dominance of expanding montmorillonite clays in the Black Vertosol, could

Table 1. Bulk soil characteristics

Soil	Depth (cm)	pH	% Mass distribution		Horizon	Colour	Texture
			>53 µm	<53 µm			
Red Chromosol	0–9	5.7	32	68	A11	10YR 4/2 dry	loam
	25–33	5.9	26	74	B1	5YR 5/8 dry	light clay
Black Vertosol	0–12.5	7	10	90	AB	10YR 3/1 moist	heavy clay
	50–90	8.1	5	95	B2	10YR 3/1 moist	heavy clay

possibly lead to differences in PyC preservation mechanisms and efficacy.

Soil pretreatment and oxidation treatments

Bulk soils were wet-sieved to <2 mm, then to <53 µm. Only the <53 µm fraction was used for subsequent treatments to isolate the oxidation-resistant fraction of organics, and the >53 µm fraction was discarded. This approach is consistent with the methods employed by Krull *et al*. (2006). Black Vertosol samples were treated with sulfuric acid to remove carbonates followed by rinsing to remove acid residues. Prior to the application of oxidation treatments, the <53 µm fraction was treated with repeated 2% HF washes to reduce the mineral content (Gonçalves *et al.* 2003) and remove organics preserved through association with mineral surfaces, and then subsequently rinsed to remove HF residues. The HF-treated <53 µm fraction is referred to as the '<53 µm fraction' in the remainder of the text.

After concentration of organics in the <53 µm fraction through treatment with HF, three different oxidative treatments were applied to subsamples of the <53 µm fraction of the four soils for isolation of oxidation-resistant organic residues: CrA (Masiello and Druffel 1998), PO (Skjemstad *et al.* 1993; Skjernstad *et al.* 1999) and a combined treatment of CrA followed by PO (CrA +PO). Briefly, the oxidative treatments were as follows: for the CrA treatment, ~2.5 g of the <53 µm fraction was exposed to repeated aliquots of 0.25 M dichromate/2 M sulfuric acid until no reaction was observed. The soluble oxidation products were removed through centrifugation and aspiration. For the PO treatment, suspensions of the <53 µm fraction were subjected to ultraviolet radiation (2.5 kW) while being flooded with oxygen from an ozone-generating 1000 V mercury vapour lamp (Oliphant OCL-1000; Oliphant UV Products, Arndell Park, NSW, Australia) for 8 h. The soluble oxidation products were removed from suspensions using Millipore immersible CX-30 ultrafiltration units (Millipore Corporation, Milford, MA, USA).

Isotopic and spectroscopic analyses

Samples were analysed for total C, total N, $\delta^{13}C$ and radiocarbon abundance both before (bulk soils and <53 µm fraction) and following chemical oxidation treatments (measurements were not replicated). Samples were graphitised and measured for radiocarbon abundance at the Center for Accelerator Mass Spectrometry at Lawrence Livermore National Laboratory in 2004. Samples were dried, weighed into quartz tubes and sealed under vacuum. Samples were combusted at 900°C for 6 h with cupric oxide and silver in sealed quartz test tubes to form carbon dioxide (CO_2) gas. The CO_2 was then reduced to graphite through heating at 570°C in the presence of hydrogen gas and a Fe catalyst (Vogel *et al.* 1987). Graphite targets were then analysed for radiocarbon abundance (Davis *et al.* 1990) and corrected for mass-dependent fractionation using measured $\delta^{13}C$ values according to Stuiver and Polach (1977). Radiocarbon abundances are expressed in units of $F^{14}C$ according to the recommendations of Reimer *et al.* (2004); analytical error was ± 0.0032 $F^{14}C$ on average. Estimated mean residence times (MRT) were calculated from $F^{14}C$ values using a time-dependent steady-state model (Trumbore 1993; Torn *et al.* 2002) populated with the atmospheric radiocarbon calibration dataset from the Southern Hemisphere calibration zone (Hogg *et al.* 2013). MRT values were rounded to the nearest decade.

Organic matter molecular structure of samples was measured by cross polarization magic angle spinning ^{13}C nuclear magnetic resonance spectroscopy and NEXAFS. The NMR data were corrected for under-representation of aryl C following Skjemstad *et al*. (2002) and Skjernstad *et al*. (1999) to allow for estimation of PyC contents (f_a). The variable f_a is the fraction of total C (as measured by NMR) which is aryl C after correction for lignin content, and was used in the current study to estimate PyC content of the samples before and following oxidation treatments. The proportional contribution of different functional groups was determined by integration of NMR spectra as follows (Wilson 1987): ketonic/aldehyde (220–190 ppm), carbonyl (190–165 ppm), O-aryl (165–140 ppm), aryl (140–110 ppm), O-alkyl (110–45 ppm) and alkyl (45–0 ppm). Assignment of peak functional groups to the relative abundance of organic compound classes was done following the molecular mixing model of Nelson and Baldock (2005). This molecular mixing model uses the C/N ratio of the sample in conjunction with the integrated peak areas of NMR spectra to express the relative abundances of different compound classes (carbohydrate, protein, lignin, aliphatic material, char and pure carbonyl).

Particle size and morphology of oxidised samples were examined using SEM/energy dispersive X-ray spectroscopy (SEM/EDAX). The NMR, SEM/EDAX and isotopic methods used are detailed in Krull *et al*. (2006).

The C and N NEXAFS spectra were obtained with a spherical grating monochromator (SGM; Regier *et al*. 2007) on beamline 11ID-1 at the Canadian Light Source at the University of Saskatchewan, Saskatoon, Canada (for C described by Heymann *et al.* 2011). Due to limitations in beamtime at the synchrotron facility, NEXAFS analysis was performed only on the surface horizon of the Black Vertosol soil. Samples were ground with mortar and pestle to increase homogenisation. The exit slit gap was 50 µm. Background measurements were taken on an empty gold (Au) wafer for each sample plate loaded into the chamber. Normalisation current was measured during each scan by collecting the total electron yield from an Au mesh. The mesh was monitored for C contamination and was periodically refreshed using an in-situ Au evaporator incorporated into the beamline vacuum system. Duplicate measurements were taken for each sample at different locations on the sample. If differences were observed, additional measurements (up to five) were taken and averaged.

The C data were background corrected using a linear regression of the pre-edge region (280–282 eV) and normalised to an edge step of one between pre- (280–282 eV) and post-edge region (300–310 eV) before curve fitting using ATHENA 0.8.052 software (Ravel and Newville 2005). The photon energy was calibrated to the C 1s → π* resonance in carbon monoxide gas at 287.38 eV. The dominant features of the C k-edge spectra include: (1) quinone and diene C at 284.5 eV, (2) aryl and olefinic C at 285.2 eV, (3) unsaturated C at 286.1 eV, (4) phenolic (aromatic C connected to O group (COH) in phenols) and ketonic C (carbonyl substituted aromatic structures of quinones, phenols and ketones)

at 286.7 eV, (5) aliphatic and carbonyl C (carbonyl functionalities from aromatic ketones) at 287.7 eV, (6) carboxylic C, carbonyl C in carboxylic acids, aromatic alcohols and polysaccharide structures at 288.4 eV, (7) O-alkyl C (e.g. alcohols and hydroxylated- and ether-linked C species) and carbonyl C (aromatic alcohols and quinine structures) at 289.1–290.0 eV.

Likewise, N data were background corrected using linear regression of the pre- and post-edge regions and normalised to an edge step of one. Normalised NEXAFS spectra were deconvoluted using a non-linear least square fitting method. Using the curve fitting application Fityk ver. 0.9.8 (Wojdyr 2010), an arctangent function was used to model the N ionisation step and fixed at 404.5 eV and spectral features resolved using Gaussian curves in the range 390–430 eV. The Gaussian curve centre and half width at half maximum (hwhm) were assigned by examining peak resonances for pure chemical standards representative of specific functional groups (Zubavichus *et al.* 2004, 2005; Leinweber *et al.* 2007; Solomon *et al.* 2009).The dominant features of the N k-edge spectra include: (1) aromatic N in six-membered rings (pyridine-like C=N) at 398.14–398.88 eV, (2) nitrilic at 399.99–400.00 eV; (3) aromatic N in five-membered rings (pyrole-like C=N) at 399.92–400.03 eV; (4) amide-N with one oxygen substitution (N–C=O) at 400.67 eV; (5) amide-N with two oxygen substitution at 401.12 eV; (6) N with unpaired electrons in five-membered rings (2N) at 401.20–401.42 eV; (7) N with unpaired electrons in five member rings (1N) at 402.13 eV; (8) N-bonded aromatic at 403.43–403.75 eV; and (9) 1s→σ* N–H transition at 405.25–412.58 eV.

Comparison of treatments was as follows: '<53 µm fraction' refers to the <53 µm fraction of bulk soil that has undergone HF treatment but no further treatment. 'CrA', 'PO' and 'CrA +PO' refer to the residues produced by subsequent oxidative treatment of this <53 µm fraction. Detailed descriptions of treatments are given in 'Soil pretreatment and oxidation treatments'. One-way analysis of variance (ANOVA) was used to assess differences in C recovery and aryl C content (as estimated by f_a values) in oxidation residues (CrA, PO and CrA+PO) in comparison with the <53 µm fraction. Due to the strong dependence of $F^{14}C$ values on soil type and depth, paired *t*-tests were used to assess differences in radiocarbon abundance (and thereby inferred mean residence time) in oxidation residues in comparison to the <53 µm fraction.

Results

Elemental and isotopic composition

C recovery

Total soil organic C was reduced by ~16–46% during separation of the <53 µm fraction and its subsequent treatment with HF. All three oxidation treatments significantly reduced C recovery in comparison to the <53 µm fraction, and the combined CrA+PO treatment reduced C recovery significantly more than CrA or PO treatments alone (one-way ANOVA, $P < 0.001$) (Fig. 1*a*, Table 2).

N and C/N ratio

No relationship between N concentration and MRT was found ($R^2 = 0.04$, $P = 0.61$). Although C/N ratios of CrA and PO treatments increased compared with the <53 µm fraction, the differences were not significant. The C/N ratios after CrA +PO treatment were significantly higher than all other treatments (one-way ANOVA, $P = 0.016$) (Fig. 1*b*, Table 2).

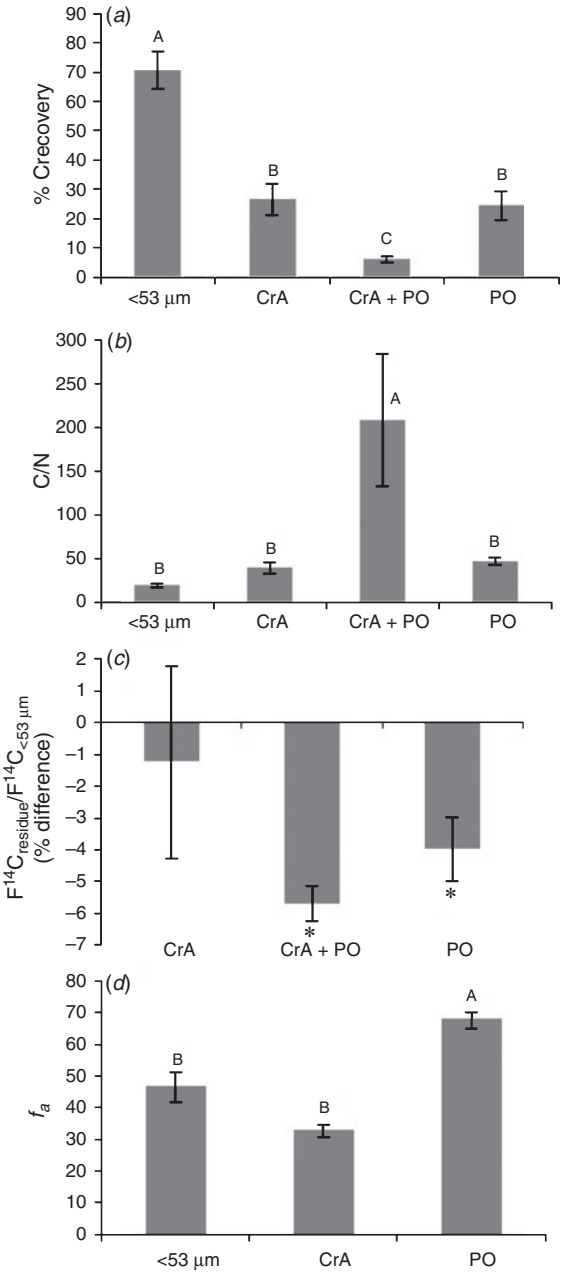

Fig. 1. (*a*) The % C recovery of the <53 µm fraction and residues following oxidation treatments relative to bulk soils. (*b*) The C/N ratios of the <53 µm fraction and residues following oxidation treatments. (*c*) Change in $F^{14}C$ values between the <53 µm fraction and the residues following treatment. Values are expressed as % change in residue relative to the >53 µm fraction. * indicates that residues were significantly depleted in comparison to the <53 µm fraction. (*d*) f_a of the <53 µm fraction and residues following treatment. Letters represent significant differences among treatments as determined by ANOVA followed by Tukey's HSD, $\alpha = 0.05$. Error bars represent the standard deviation of four replicates for each treatment. The CrA+PO treatment is not shown because it was only measured on two of the four samples.

Table 2. Elemental and isotopic data for bulk soils and isolated fractions
n.d., no data

Soil	Depth (cm)	Treatment	$F^{14}C$	MRT (years)	%C recovery[A]	%C	%N	C/N	$\delta^{13}C$
Red Chromosol	0–9	Bulk soil	0.9629	280		4.65	0.19	25	–21.2
		<53 μm	0.9985	30	54.2	42.20	1.93	22	–20.5
		CrA	0.9344	550	26.6	21.50	0.53	40	–22.9
		CrA+PO	0.9285	600	5.2	19.20	0.13	153	–23.7
		PO	0.9412	480	19.9	33.10	0.59	56	–24.1
	25–33	Bulk soil	0.8725	1170		0.80	0.04	20	–19.9
		<53 μm	0.8318	1620	84.3	15.40	1.03	15	–20.8
		CrA	0.8935	950	11.8	4.35	0.18	24	–23.6
		CrA+PO	0.7923	2100	4.5	3.00	0.02	134	–25.6
		PO	0.7965	2050	18.4	8.70	0.21	42	–24.8
Black Vertosol	0–12.5	Bulk soil	0.9006	950		2.15	0.14	15	–15.2
		<53 μm	0.8801	1090	71.5	38.20	2.65	14	–14.9
		CrA	0.8591	1310	30.5	17.00	0.49	35	–15.0
		CrA+PO	0.8379	1550	5.6	11.10	0.03	436	–13.9
		PO	0.8700	1190	20.2	23.70	0.61	39	–14.2
	50–90	Bulk soil	0.6881	3640		1.50	0.07	23	–12.3
		<53 μm	0.6933	3550	72.8	33.90	1.51	23	n.d.
		CrA	0.6682	3990	36.9	17.30	0.30	57	–12.9
		CrA+PO	0.6500	4320	9.0	14.00	0.13	111	–12.6
		PO	0.6603	4130	38.7	29.60	0.61	49	–12.6

[A]Relative to bulk soil.

Stable isotopes

The $\delta^{13}C$ values for the Red Chromosol oxidative residues suggest that the majority of organic inputs originated from C_3 plants, most likely eucalyptus trees. In contrast, at the more grass-dominated Black Vertosol site, oxidative residues had $\delta^{13}C$ values resembling C_4 vegetation, indicating a difference in fire fuels between the two soils. Missing datapoints made quantitative comparisons of $\delta^{13}C$ impossible, but $\delta^{13}C$ values show a general trend of depletion with oxidative treatment in Red Chromosol soils. This trend was not evident in Black Vertosol soils (Table 2).

Radiocarbon abundance

The $F^{14}C$ values generally decreased with oxidative treatment compared with both bulk soils and the <53 μm fraction (Table 2), but differences were not always significant. The $F^{14}C$ values of the <53 μm fraction were not significantly depleted in comparison to bulk soils (paired *t*-test, two-tailed $P = 0.778$). The CrA treatment alone did not significantly decrease $F^{14}C$ values in comparison to bulk soils (paired *t*-test, two-tailed $P = 0.292$), but reductions were evident in the combined CrA+PO. The PO treatment showed some evidence of reduced $F^{14}C$ values (paired *t*-test, two-tailed $P = 0.052$). In comparison to the <53 μm fraction, CrA again did not significantly influence $F^{14}C$ values (paired *t*-test, two-tailed $P = 0.678$), whereas PO and CrA+PO significantly decreased $F^{14}C$ values in both soil types (paired *t*-tests, two-tailed $P = 0.039$ and 0.006 respectively). Because of the strong influence of depth and soil type on $F^{14}C$ values (Table 2), data were displayed as the difference between $F^{14}C$ values of the <53 μm and the respective treatments (Fig. 1*c*). Supplementary radiocarbon information is provided in Table S4.

NMR and NEXAFS: molecular structure measurements

NMR analysis

The PO and CrA+PO treatments produced residues enriched in aryl C in comparison to the <53 μm fraction, and PO residues were significantly more enriched in aryl C than CrA residues (Fig. 1*d*) (one-way ANOVA, $P < 0.001$). The CrA treatment resulted in residues enriched in alkyl C in comparison to both the <53 μm fraction and the PO treatment residues (one-way ANOVA, $P < 0.001$). The CrA treatment resulted in a relative depletion of carbohydrates and proteins concomitant with relative enrichment of lipids. In contrast, PO treatment resulted in relative enrichment of PyC and depletion of proteins, carbohydrates and lipids (Fig. 2, Table S1).

NEXAFS analysis

The C NEXAFS data confirmed a concentration of aromatic C structures in the PO and CrA+PO treatments, with notable relative enrichment of phenolic C and decreases in aliphatic, carboxylic and alkyl C. Unsaturated C was enriched in all three treatments in comparison to the <53 μm fraction, but the most notable increase was in the PO treatment. The C NEXAFS spectra did not show the relative enrichment in aliphatic C post-CrA treatment that was indicated by NMR analysis, most likely because NEXAFS did not have a strong well-defined feature in that region (Fig. 3*a*, Table S2).

The N NEXAFS spectra (Fig. 3*b*, Table S3) indicated that the <53 μm fraction comprised mainly heterocyclic N, both pyrroles and pyridines. It also contained a relatively high concentration of N bonded to aromatic rings, followed by a small proportion of amide bonds. The PO treatment seemed to substantially degrade the overall structure of the N pool, leaving few distinctive absorption bands in either the PO or the CrA+PO

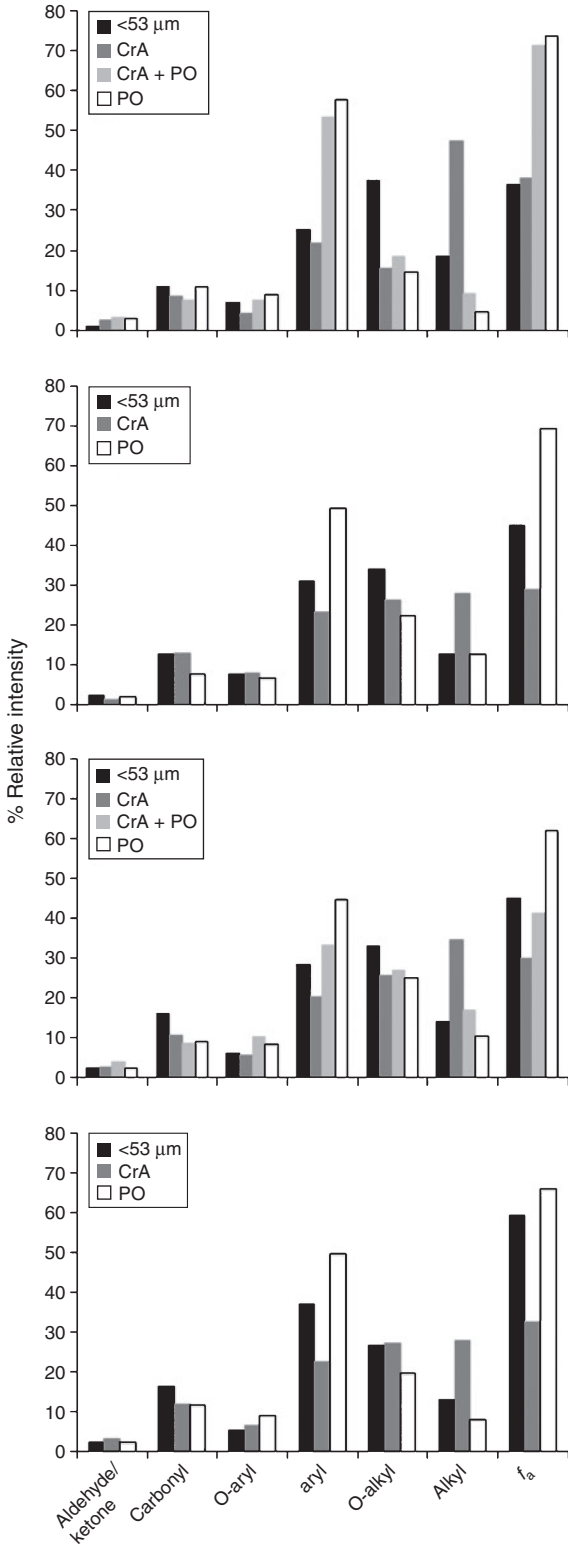

Fig. 2. Relative intensity of integrated functional group areas derived from ^{13}C-NMR spectra. Corresponding spectral ranges in ppm are given in Table S1. The variable f_a is the fraction of total C (as measured by NMR) which is aryl C after correction for lignin content, and is used in the current study to estimate PyC content of the samples before and following oxidation treatments.

spectra. However, when the absorbance bands were deconvoluted, pyrroles, nitrile N and N bonded to aromatics were present in higher proportions than any other form of N. Following CrA treatment, the relative proportion of pyrrole N (C–N bond) increased, accompanied by a relative decrease in the proportion of pyridines.

SEM/EDAX analysis

The SEM images of the CrA and PO treatment residues are shown in Fig. 4. Notably, although spectrometry data indicated significant differences in molecular composition between the oxidative treatments, SEM images did not indicate differences in particle size or appearance. Images feature blocky, plant-like particles with fractured edges, which are characteristics of finely divided soil char fragments (Skjemstad *et al.* 2002) as well as finer residue. EDAX data indicated an average C content of 70 atom % and average O content of 10–25 atom % in the examined areas (data not shown), suggesting that the vast majority of the particles were organic, not mineral.

Discussion

(*1*) *How do soil morphology and fire fuel type influence charcoal persistence in soils, if at all?*

Contrary to our hypothesis, neither vegetation type nor soil morphology significantly influenced PyC abundance or persistence in the two soils examined. The Black Vertosol, assumed to have a lower protective capacity for particulate PyC due to disruption of aggregates associated with self-mulching, was consistently radiocarbon-depleted in comparison to the Red Chromosol soil. We expected that PyC produced though grassland fires would be finer-grained and less condensed in comparison to PyC formed from wood (Graetz and Skjemstad 2003). However, although δ^{13}C values confirmed that oxidative residues from the two sites differed in their sources (wood vs grass), the abundance and characteristics of the oxidative residues were highly similar between the sites. Given the similarity of the residues between the two sites, an explanation for why the Black Vertosol residues were consistently older than the Red Chromosol residues is not immediately forthcoming. It is possible that due to its fluvial nature, the Black Vertosol soil had been truncated in the recent past. It is also possible that poor drainage conditions associated with Black Vertosol soils could lead to reductions in biodegradation of SOM, or that the finer texture of the Black Vertosol actually acted as an effective stabilisation mechanism.

(*2*) *Is N concentration or N functional group composition a significant factor in explaining PyC mean residence time?*

The N concentration was not a determining factor in oxidative residue MRT, suggesting that increasing N concentration did not make oxidative-resistant SOM more desirable as a microbial substrate. Although the relative proportion of total N concentrations in the CrA and PO residues was similar, NEXAFS data suggested that the structure of the N compounds differed between the two treatments. The CrA oxidation seemed to preferentially break down pyridine and N-bonded aromatics but had no effect on pyrroles. Pyridines

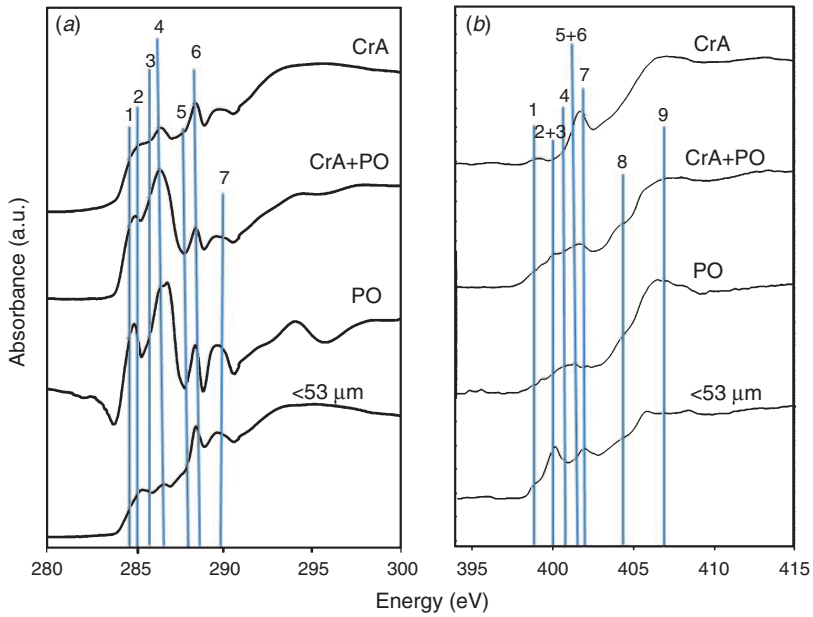

Fig. 3. (*a*) C NEXAFS spectra for the Black Vertosol 0–12.5 cm sample. Peak assignments are as follows: (1) quinone and diene C at 284.5 eV, (2) aryl and olefinic C at 285.2 eV, (3) unsaturated C at 286.1 eV, (4) phenolic (aromatic-C connected to O group (COH) in phenols) and ketonic C (carbonyl substituted aromatic structures of quinones, phenols and ketones) at 286.7 eV, (5) aliphatic and carbonyl C (carbonyl functionalities from aromatic ketones) at 287.7 eV, (6) carboxylic C, carbonyl C in carboxylic acids, aromatic alcohols and polysaccharide structures at 288.4 eV, (7) O-alkyl C (e.g. alcohols and hydroxylated- and ether-linked C species) and carbonyl C (aromatic alcohols and quinine structures) at 289.1–290.0 eV. (*b*) N NEXAFS spectra for the Black Vertosol 0–12.5 cm sample. Peak assignments are as follows: (1) aromatic N in six-membered rings (pyridine-like C=N) at 398.14–398.88 eV, (2) nitrilic at 399.99–400.00 eV, (3) aromatic N in five-membered rings (pyrole-like C=N) at 399.92–400.03 eV, (4) amide-N with one oxygen substitution (N–C=O) at 400.67 eV, (5) amide-N with two oxygen substitution at 401.12 eV, (6) N with unpaired electrons in five-membered rings (2N) at 401.20–401.42 eV, (7) N with unpaired electrons in five member rings (1N) at 402.13 eV, (8) N-bonded aromatic at 403.43–403.75 eV and (9) 1s→σ* N–H transition at 405.25–412.58 eV.

were sensitive to oxidative treatment by PO but N-bonded aromatics were not. The presence of nitriles in the PO treatment compared with <53 µm suggest a transformation of amines or amides via oxidation. Also, although the CrA+PO treatment showed a significant loss of N compared with the CrA and PO treatments, as well as a significant increase in MRT, the actual structure of the N compounds in the CrA+PO residue was similar to the PO residue. The highly degraded nature of the N NEXAFS spectra in the PO and CrA+PO residues suggests that N-containing moieties of all structural types were sensitive to photo-oxidation, whereas CrA affected mostly aromatic structures. The results did not support the hypothesis that N functional group composition influences the MRT of the oxidative-resistant fraction of SOM.

Interpretations of functional group composition of fractions must be done with caution, as the oxidative separation itself may have changed surface properties. However, such surface oxidation is here assumed to be small compared with the bulk properties, as even strong surface oxidation found by Cheng *et al*. (2008) was not detectable after grinding and exposing the much larger interior mass of PyC particles.

(*3*) *Can connections be made between oxidative resistance, molecular structure and persistence of PyC fractions in soils?*

Previous work on similar soils (Krull *et al.* 2006) suggested that oxidative resistance was not a reliable proxy for SOM persistence in soils with high fire-frequency since the most strongly oxidising treatments sometimes produced highly aromatic residues (assumed to be charcoal), which were enriched in radiocarbon in comparison to the bulk soil. This suggested that the oxidative resistance of charcoal may decrease with increasing residence time in soil. Additionally, Krull *et al*. (2006) speculated that because different oxidative/hydrolytic treatments produced residues with unique molecular composition and radiocarbon signature, it may be possible to separate out distinct generations of PyC in a bulk soil through careful selection of oxidative treatments.

Results of the current study offer contrasting conclusions. Both the Red Chromosol and Black Vertosol sample sites were located in regions of decadal burning frequency, yet the ‘PyC isolation’ treatments applied to the soils yielded residues with

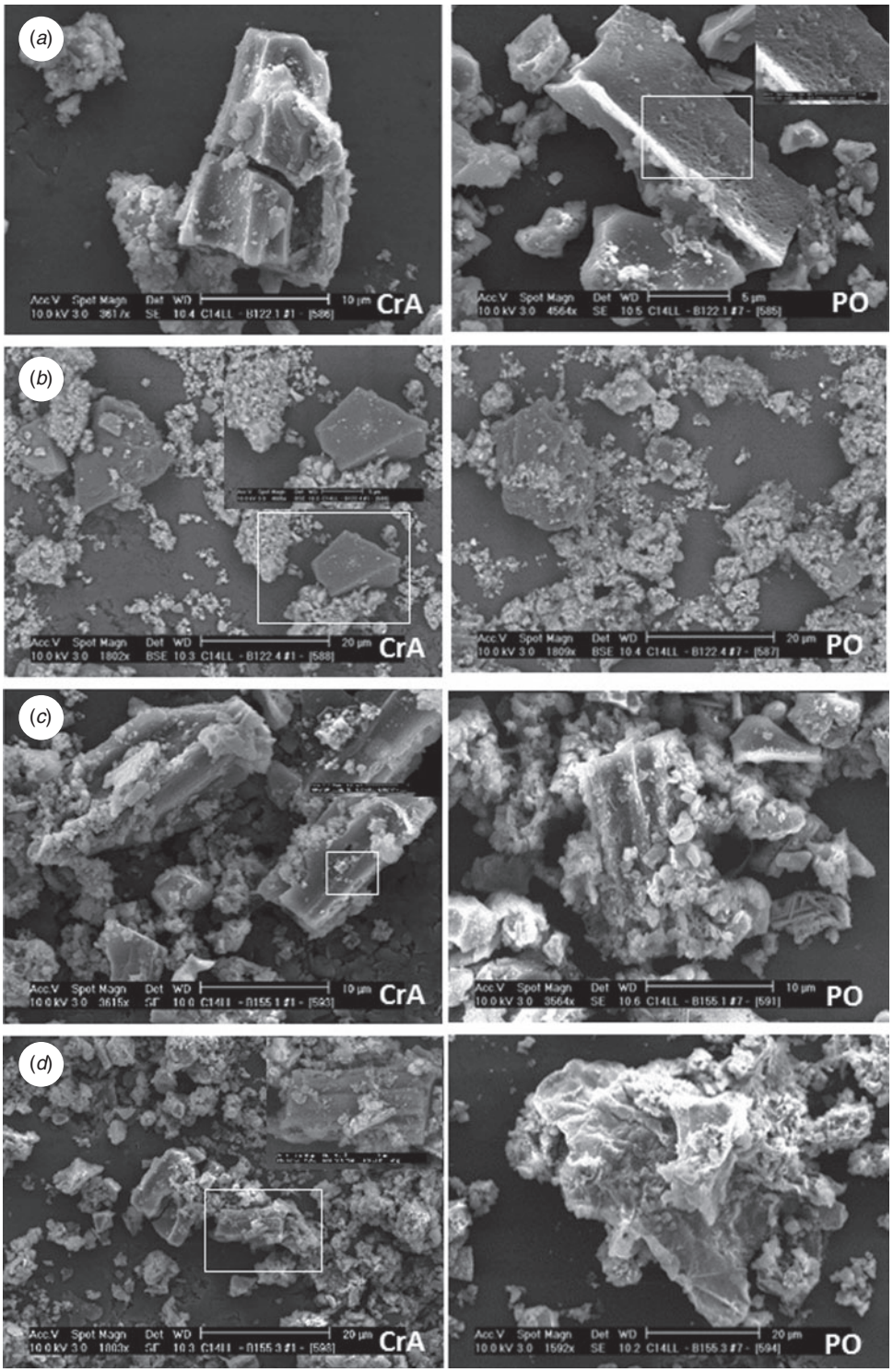

Fig. 4. Scanning electron microscopy images following CrA and PO treatment of (*a*) Red Chromosol, 0–9 cm sample, (*b*) Red Chromosol, 25–33 cm sample, (*c*) Black Vertosol, 0–12.5 cm sample, (*d*) Black Vertosol, 50–90 cm sample. White boxes indicate the portion of the figure that is shown in higher resolution.

MRTs on the order of hundreds to a few thousands of years. If it were simply the highly condensed aromaticity of PyC materials that provided the persistence of the PyC input and oxidative resistance of the 'passive' fraction of SOM, then the most aromatic fraction would not necessarily be the oldest fraction because of frequent inputs of fresh pyrogenic

materials. Indeed the most structurally 'recalcitrant' (highly condensed aromatic) fraction could then have any radiocarbon signature, and the radiocarbon signature would more reflect fire frequency than the actual MRT of the pyrogenic materials in the soil, as discussed by Krull *et al*. (2006). However, in the majority of cases in the current dataset, the oxidative residues had significantly depleted $F^{14}C$ signatures (i.e. longer average MRTs) in comparison to bulk soils and the <53 µm fraction (Fig. 1*c*). This is partially the result of removal of non-PyC during sieving, HF treatment and oxidative treatment, but it also suggests that newly formed pyrogenic materials from more recent fire events were more susceptible to the oxidation treatments applied here than materials that had been residing in the soil for hundreds to several thousands of years. This result is in contrast to the findings of Krull *et al*. (2006), which indicated that CrA+PO treatment could isolate a recently created charcoal pool in a soil with high burn frequency.

Although CrA and PO are both methods designed to isolate the most oxidation-resistant fraction of SOM, the chemical nature of the residues is necessarily a reflection of the interaction of the treatment applied with the chemical nature of the organic matter being subjected to treatment. As in Krull *et al*. (2006), CrA seemed to attack aromatics, perhaps removing older 'weathered' PyC and selecting for non-acid soluble structures, hence the enrichment in lipids in CrA residues. In contrast, PO targets low energy bonds which are easily radicalised and subsequently oxidised, thereby preserving aromatic and C=C double bonds regardless of age (Lagercrantz and Yhland 1963; Slawinska *et al.* 1975; Senesi and Schnitzer 1977; Zepp *et al.* 1977). The two methods therefore target different classes of molecular structures and result in residues with differing chemical composition which is reflected in NMR and NEXAFS spectra (Figs 2, 3).

Radiocarbon abundance (and by extension, MRT in the soil) varied among oxidative treatments. Whether these differences in average MRT reflect differences in molecular structure cannot be determined with any certainty due to the limited size of the current dataset. However, it should be noted that the combined CrA+PO treatment consistently isolated the fraction with the longest average MRT, and the molecular structure of this residue was intermediate in character between the CrA- and PO-only residues (Figs 1*c*, 2, 3). This implies that the most oxidatively resistant and oldest fraction of <53 µm SOM in these highly fire-affected soils was not composed solely of highly condensed aromatic structures but was a mix of aliphatic and aromatic compounds.

Conclusions

The CrA and PO treatments isolate chemically distinct pools of SOM, which are structurally consistent with the respective qualities of the extractants. The CrA+PO treatment produced an organic residue that was structurally most similar to the PO treatment, but also contained a substantial alkyl component, and additionally had the longest average MRT. These results suggest that both aromaticity and hydrophobicity/insolubility play a role in the persistence of what is often isolated as the 'passive' fraction of SOM, and that even in soils that are burnt frequently, the most persistent SOM pool is not solely composed of PyC materials.

Supplementary material

NMR and NEXAF spectral areas and radiocarbon supplementary information are available from the Journal's website.

Acknowledgements

We acknowledge funding support by CSIRO and USDA (No. 2008–35615–18961). We are grateful for the support by Tom Regier at the SGM beamline of the Canadian Light Source. We acknowledge the substantial efforts and input of Evelyn Krull, formerly of CSIRO Land & Water. We also wish to acknowledge the comments and revisions suggested by the associate editor and two anonymous reviewers of *Soil Research*, which substantially improved the quality of this manuscript.

References

Bird MI, Wynn JG, Saiz G, Wurster CS, McBeath A (2015) The pyrogenic carbon cycle. *Annual Review of Earth and Planetary Sciences* **43**, 273–298. doi:10.1146/annurev-earth-060614-105038

Cheng CH, Lehmann J, Engelhard M (2008) Natural oxidation of black carbon in soils: changes in molecular form and surface charge along a climosequence. *Geochimica et Cosmochimica Acta* **72**, 1598–1610. doi:10.1016/j.gca.2008.01.010

Cohen-Ofri I, Weiner L, Boaretto E, Mintz G, Weiner S (2006) Modern and fossil charcoal: aspects of structure and diagenesis. *Journal of Archaeological Science* **33**, 428–439. doi:10.1016/j.jas.2005.08.008

Czimczik CI, Masiello CA (2007) Controls on black carbon storage in soils. *Global Biogeochemical Cycles* **21**, GB3005. doi:10.1029/2006GB002798

Davis JC, Proctor ID, Southon JR, Caffee MW, Heikkinen DW, Roberts ML, Moore TL, Turteltaub KW, Nelson DE, Loyd DH, Vogel JS (1990) LLNL/US AMS facility and research program. *Nuclear Instruments and Methods in Physics Research Section B: Beam Interactions with Materials and Atoms* **52**, 269–272. doi:10.1016/0168-583X(90)90419-U

Gonçalves CN, Dalmolin RSD, Dick DP, Knicker H, Klamt E, Kögel-Knabner I (2003) The effect of 10% HF treatment on the resolution of CPMAS ^{13}C NMR spectra and on the quality of organic matter in Ferralsols. *Geoderma* **116**, 373–392. doi:10.1016/S0016-7061(03)00119-8

González-Pérez J, González-Vila FJ, Almendros G, Knicker H (2004) The effect of fire on soil organic matter—a review. *Environment International* **30**, 855–870. doi:10.1016/j.envint.2004.02.003

Graetz RD, Skjemstad JO (2003) The charcoal sink of biomass burning on the Australian continent. Atmospheric Research Technical Paper 64. CSIRO, Aspendale, Victoria, Australia. Available at http://www.cmar.csiro.au/e-print/open/graetz_2003a.pdf [verified 5 June 2017].

Hammes K, Schmidt MWI, Smernik RJ, Currie LA, Ball WP, Nguyen TH, Louchouarn P, Houel S, Gustafsson Ö, Elmquist M, Cornelissen G, Skjemstad JO, Masiello CA, Song J, Peng P, Mitra S, Dunn JC, Hatcher PG, Hockaday WC, Smith DM, Hartkopf-Fröder C, Böhmer A, Lüer B, Huebert BJ, Amelung W, Brodowski S, Huang L, Zhang W, Gschwend PM, Xanat Flores-Cervantes D, Largeau C, Rouzaud J-N, Rumpel C, Guggenberger G, Kaiser K, Rodionov A, Gonzalez-Vila FJ, Gonzalez-Perez JA, de la Rosa JM, Manning DAC, López-Capél E, Ding L (2007) Comparison of quantification methods to measure fire-derived (black/elemental) carbon in soils and sediments using reference materials from soil, water, sediment and the atmosphere. *Global Biogeochemical Cycles* **21**, GB3016. doi:10.1029/2006GB002914

Heymann K, Lehmann J, Solomon D, Schmidt MWI, Regier T (2011) C 1s K-edge near-edge X-ray absorption fine structure (NEXAFS) spectroscopy for characterizing the functional group chemistry of black carbon. *Organic Geochemistry* **42**, 1055–1064. doi:10.1016/j.orggeochem.2011.06.021

Hogg AG, Hua Q, Blackwell PG, Buck CE, Guilderson TP, Heaton TJ, Niu M, Palmer JG, Reimer PJ, Reimer RW, Turney CSM, Zimmerman SRH (2013) SHCal 13 southern hemisphere calibration, 0–50,000 years cal BP. *Radiocarbon* **55**, 1–15.

Isbell RF (2002). 'The Australian soil classification.' Revised edn. (CSIRO Publishing: Collingwood, Victoria)

Knicker H (2007) How does fire affect the nature and stability of soil organic nitrogen and carbon? A review. *Biogeochemistry* **85**, 91–118. doi:10.1007/s10533-007-9104-4

Knicker H (2011*a*) Pyrogenic organic matter in soil: its origin and occurrence, its chemistry and survival in soil environments. *Quaternary International* **243**, 251–263. doi:10.1016/j.quaint.2011.02.037

Krull ES, Swanston CW, Skjemstad JO, McGowan JA (2006) Importance of charcoal in determining the age and chemistry of organic carbon in surface soils. *Journal of Geophysical Research* **111**, G04001. doi:10.1029/2006JG000194

Lagercrantz C, Yhland M (1963) Photo-induced free radical reactions in the solutions of some tars and humic acids. *Acta Chemica Scandinavica* **17**, 1299–1306. doi:10.3891/acta.chem.scand.17-1299

Leavitt SW, Follett RF, Paul EA (1996) Estimation of slow- and fast-cycling soil organic carbon pools from 6N HCl hydrolysis. *Radiocarbon* **38**, 231–239. doi:10.1017/S0033822200017604

Leinweber P, Kruse J, Walley FL, Gillespie A, Eckhardt K-U, Blyth RIR, Regier T (2007) N K-edge XANES: an overview of reference compounds used to identify 'unknown' organic nitrogen in environmental samples. *Journal of Synchrotron Radiation* **14**, 500–511. doi:10.1107/S0909049507042513

Martel YA, Paul EA (1974) The use of radiocarbon dating of organic matter in the study of soil genesis. *Soil Science Society of America Proceedings* **38**, 501–506. doi:10.2136/sssaj1974.03615995003800030033x

Masiello CA, Druffel ERM (1998) Black carbon in deep-sea sediments. *Science* **280**, 1911–1913. doi:10.1126/science.280.5371.1911

Nelson PN, Baldock JA (2005) Estimating the molecular composition of a diverse range of natural organic materials from solid-state ^{13}C NMR and elemental analysis. *Biogeochemistry* **72**, 1–34. doi:10.1007/s10533-004-0076-3

Ravel B, Newville M (2005) ATHENA, ARTEMIS, HEPHAESTUS: data analysis for x-ray absorption spectroscopy using IFEFFIT. *Journal of Synchrotron Radiation* **12**, 537–541. doi:10.1107/S0909049505012719

Regier T, Krochak J, Sham TK, Hu YF, Thompson J, Blyth RIR (2007) Performance and capabilities of the Canadian Dragon: The SGM beamline at the Canadian Light Source. *Nuclear Instruments and Methods in Physics Research Section A: Accelerators, Spectrometers, Detectors and Associated Equipment* **582**, 93–95.

Reimer PJ, Brown TA, Reimer RW (2004) Discussion: reporting and calibration of post-bomb C-14 data. *Radiocarbon* **46**, 1299–1304. doi:10.1017/S0033822200033154

Schmidt MWI, Noack AG (2000) Black carbon in soils and sediments: analysis, distribution, implication, and current challenges. *Global Biogeochemical Cycles* **14**, 777–793. doi:10.1029/1999GB001208

Schmidt MWI, Skjemstad JO, Czimczik CI, Glaser B, Prentice KM, Gelinas Y, Kuhlbusch TAJ (2001) Comparative analysis of black carbon in soils. *Global Biogeochemical Cycles* **15**, 163–167. doi:10.1029/2000GB001284

Senesi N, Schnitzer M (1977) Effects of pH, reaction time, chemical reduction and irradiation on the ESR spectra of fulvic acid. *Soil Science* **123**, 224–234. doi:10.1097/00010694-197704000-00003

Skjemstad JO, Janic LJ, Head MJ, McClure SG (1993) High energy ultraviolet photo-oxidation: a novel technique for studying physically protected organic matter in clay- and silt-sized aggregates. *Journal of Soil Science* **44**, 485–499. doi:10.1111/j.1365-2389.1993.tb00471.x

Skjemstad JO, Clarke P, Taylor JA, Oades JM, McClure SG (1996) The chemistry and nature of protected carbon in soil. *Soil Research* **34**, 251–271.

Skjemstad JO, Reicosky DC, Wilts AR, McGowan JA (2002) Charcoal carbon in U.S. agricultural soils. *Soil Science Society of America Journal* **66**, 1249–1255. doi:10.2136/sssaj2002.1249

Skjernstad JO, Taylor JA, Smernik RJ (1999) Estimation of charcoal (char) in soils. *Communications in Soil Science and Plant Analysis* **30**, 2283–2298. doi:10.1080/00103629909370372

Slawinska D, Slawinska J, Sarna T (1975) The effect of light on the ESR spectra of humic acids. *Journal of Soil Science* **26**, 93–99. doi:10.1111/j.1365-2389.1975.tb01934.x

Solomon D, Lehmann J, Kinyangi J, Liang B, Hanley K, Heymann K, Wirick S, Jacobsen C (2009) Carbon (1s) NEXAFS spectroscopy of biogeochemically relevant organic reference compounds. *Soil Science Society of America Journal* **73**, 1817–1830. doi:10.2136/sssaj2008.0228

Song J, Peng P, Huang W (2002) Black Carbon and Kerogen in soils and sediments. 1. Quantification and characterization. *Environmental Science & Technology* **36**, 3960–3967. doi:10.1021/es025502m

Stuiver M, Polach HA (1977) Discussion: reporting of ^{14}C data. *Radiocarbon* **19**, 355–363. doi:10.1017/S0033822200003672

Torn MS, Lapenis AG, Timofeev A, Fischer ML, Babikov BV, Harden JW (2002) Organic carbon and carbon isotopes in modern and 100-year-old-soil archives of the Russian steppe. *Global Change Biology* **8**, 941–953. doi:10.1046/j.1365-2486.2002.00477.x

Trumbore SE (1993) Comparison of carbon dynamics in tropical and temperate soils using radiocarbon measurements. *Global Biogeochemical Cycles* **7**, 275–290. doi:10.1029/93GB00468

Vogel JS, Southon JR, Nelson DE (1987) Catalyst and binder effects in the use of filamentous graphite for AMS. *Nuclear Instruments and Methods in Physics Research Section B: Beam Interactions with Materials and Atoms* **29**, 50–56. doi:10.1016/0168-583X(87)90202-3

Wilson MA (1987) 'NMR techniques and applications in geochemistry and soil chemistry.' (Elsevier: New York)

Wojdyr M (2010) Fityk: a general-purpose peak fitting program. *Journal of Applied Crystallography* **43**, 1126–1128. doi:10.1107/S0021889810030499

Zepp RG, Wolfe NL, Baughman GL, Hollis RC (1977) Singlet oxygen in natural waters. *Nature* **267**, 421–423. doi:10.1038/267421a0

Zubavichus Y, Fuchs O, Weinhardt L, Heske C, Umbach E, Denlinger JD, Grunze M (2004) Soft X-ray-induced decomposition of amino acids: an XPS, mass spectrometry, and NEXAFS study. *Radiation Research* **161**, 346–358. doi:10.1667/RR3114.1

Zubavichus Y, Shaporenko A, Grunze M, Zharnikov M (2005) Innershell absorption spectroscopy of amino acids at all relevant absorption edges. *The Journal of Physical Chemistry A* **109**, 6998–7000. doi:10.1021/jp0535846